The Thirty-Third AAAI Conference on Artificial Intelligence (AAAI-19)

Interpretable Predictive Modeling for Climate Variables with Weighted Lasso

Sijie He,[1] Xinyan Li,[1] Vidyashankar Sivakumar,[1] Arindam Banerjee[1]
[1]Depertment of Computer Science & Engineering
University of Minnesota, Twin Cities
Minneapolis, MN 55455
hexxx893@umn.edu, lixx1166@umn.edu, sivak017@umn.edu, banerjee@cs.umn.edu

Abstract

An important family of problems in climate science focus on finding predictive relationships between various climate variables. In this paper, we consider the problem of predicting monthly deseasonalized land temperature at different locations worldwide based on sea surface temperature (SST). Contrary to popular belief on the trade-off between (a) simple interpretable but inaccurate models and (b) complex accurate but uninterpretable models, we introduce a weighted Lasso model for the problem which yields interpretable results while being highly accurate. Covariate weights in the regularization of weighted Lasso are pre-determined, and proportional to the spatial distance of the covariate (sea surface location) from the target (land location). We establish finite sample estimation error bounds for weighted Lasso, and illustrate its superior empirical performance and interpretability over complex models such as deep neural networks (Deep nets) and gradient boosted trees (GBT). We also present a detailed empirical analysis of what went wrong with Deep nets here, which may serve as a helpful guideline for application of Deep nets to small sample scientific problems.

Introduction

Over the past decade climate datasets with improved spatial resolutions have become available. While such datasets come from a mix of real observations and physics based models, recent years have seen considerable interest in applying machine learning techniques for predictive modeling of climate variables of interest. Such models have the potential to aid a better understanding of the impact of climate change and attribution of observed events as well as guide decision/policy making in a variety of domains such as agricultural planning, water resource management, and extreme weather events (O'Brien et al. 2006).

We consider one such problem in climate science of identifying predictive relationships between ocean sea surface temperature (SST) and land temperature (Steinhaeuser, Chawla, and Ganguly 2011a). Recent work has shown sparse modeling techniques like Lasso (Chatterjee et al. 2012) tend to better capture predictive relationships between SST and land climate compared to more traditional methods like principal component regression (PCR) (Francis and Renwick 1998), shallow neural networks (Steinhaeuser, Chawla, and Ganguly 2011b), etc. From a climate science perspective, parsimony in variable selection leads to more interpretable models helping climate scientists gain a better understanding of the underlying relationships between climate variables. Still, there are difficulties in explaining the relationships due to the variable selection inconsistency of Lasso and the high spatial correlation among SST variables.

In this paper, inspired by the adaptive Lasso (Zou 2006), we propose a weighted ℓ_1 regularized model suitable for spatial problems since it encourages the estimator to pick spatially contiguous SST covariates. The weighted ℓ_1 regularizer penalizes different components of regression coefficients θ differently and is mathematically defined by $R(\theta) = \sum_{i=1}^{p} w_i|\theta_i|$, where w_i is the weight for component i. Lower the weight, lower is the penalization on the corresponding covariates and consequently more are the chances they will be nonzero. Note that, adaptive Lasso is weighted Lasso, where the weights are chosen to be inversely proportional to the estimated coefficients from estimator like ordinary least squares (OLS). For the problem we consider, we propose the weights on ocean locations are directly proportional to their distance from the land location thus penalizing faraway ocean regions more, which is consistent with domain knowledge in climate science. We show that the weighted Lasso, in contrast to Lasso, gives more interpretable results which conform to the observations of nearby ocean locations having the most effect on land temperature.

We perform extensive comparison of the weighted Lasso with baselines on data from 3 different Earth System Models (ESMs) (Taylor, Stouffer, and Meehl 2012). First, comparisons between weighted Lasso and Lasso shows that they achieve similar predictive performance, but weighted Lasso is considerably more interpretable in terms of variable selection. Second, somewhat surprisingly, we illustrate that weighted Lasso persistently outperforms Deep nets which form the state-of-the-art in many other application areas (Krizhevsky, Sutskever, and Hinton 2012; He et al. 2016; LeCun, Bengio, and Hinton 2015); weighted Lasso is also illustrated to have superior performance over gradient boosted trees (Chen and Guestrin 2016) and PCR (Jolliffe 2011). We also present a detailed analysis of the poor performance of Deep nets and report results on a variety of settings such as number of layers, number of hidden units, mini-batch size, regularization type, etc. The key factor limiting the performance is sample size. Deep nets overfit the training set leading to poor validation/test performance. The results emphasize the need for caution and further work on Deep nets for small sample (scientific) problems.

Our main contributions in this paper are as follows:

1. We suggest the weighted Lasso estimator, which incorporates domain knowledge for finding relationships in spatial data. We also derive non-asymptotic parameter estimation error bounds for the weighted Lasso estimator.
2. We show that weighted Lasso achieves high prediction accuracy and consistent variable selection for land climate prediction using SST compared to other latest state-of-the-art machine learning methods like Deep nets and gradient boosted trees.
3. We perform extensive experiments with Deep nets and show that Deep nets easily overfit the training data without sufficient samples.

Organization of the paper: We start with a discussion on related work. We then give finite sample estimation error bounds for weighted Lasso. We subsequently present experimental results comparing the weighted Lasso with baseline methods along with in-depth results on Deep nets.

Related work

We briefly review the statistical models used in the climate sciences to discover predictive relationships between climate variables. Most statistical models perform some form of dimensionality reduction due to the large spatial datasets and relatively fewer data samples. A popular method is principal component regression (PCR) (Olivieri 2018), which has been used for temperature and precipitation prediction in New Zealand (Francis and Renwick 1998). In (Hsieh and Tang 1998), principal component analysis (PCA) is used to compress large spatial fields followed by fitting a neural network on the compressed dataset. In (Steinhaeuser, Chawla, and Ganguly 2011a) clustering is used for dimension reduction followed by various regression methods, such as linear regression, support vector regression, regression trees, to predict land temperature and precipitation from global SST field. In contrast (Chatterjee et al. 2012) model the same problem in (Steinhaeuser, Chawla, and Ganguly 2011a) as a high-dimensional sparse regression problem where the land climate is the dependent variable, SST field are the independent variables and a sparsity promoting regularizer captures the constraint that land temperature is influenced by only a few ocean locations. More recently a spectral nonlinear dimensionality reduction method is used in (DelSole and Banerjee 2017) to capture the relationship between summer Texas area temperature and Pacific SST.

Geostatistical methods, like kriging (Goovaerts 1999) and its variations have been applied for spatial interpolation of climate variables (Aalto et al. 2013). However, such methods usually only perform well within a defined local neighborhood (Walter et al. 2001). Morevover the success of such methods relies on proper choice of kernels and hyperparameters which is statistically and computationally challenging in high-dimensional datasets.

There is increasing interest in exploring the application of Deep nets in climate applications inspired by their success in domains like image processing (He et al. 2016), speech recognition (LeCun, Bengio, and Hinton 2015), etc. Recent work explore the use of Deep nets for prediction of the Oceanic Niño Index (ONI) (McDermott and Wikle 2017) and for statistical downscaling of climate variables (Vandal et al. 2017), although there is currently lacking an understanding or comprehensive study on the generalization performance of Deep nets on small sample size datasets routinely found in climate science applications.

Estimation Error Bound for Weighted Lasso

For land climate prediction using SST, the spatial information can be considered while designing the predictive models. Since land temperature is known to be mostly influenced by nearby ocean locations, we propose a modification of the weighted ℓ_1 regularizer used in weighted Lasso. It penalizes differently for temperature at each ocean location based on their distance from land target region.

In this section, we provide the non-asymptotic estimation error bound for the following weighted Lasso estimator in a general setting,

$$\hat{\theta} = \underset{\theta \in \mathbb{R}^p}{\operatorname{argmin}} \frac{1}{2n} \|y - X\theta\|_2^2 + \lambda \sum_{i=1}^{p} w_i |\theta_i| \qquad (1)$$

where, for our application, $y \in \mathbb{R}^n$ is the land temperature, $X \in \mathbb{R}^{n \times p}$ are SST at p ocean locations, $\theta \in \mathbb{R}^p$ are regression coefficients, θ_i is the ith coefficient in θ, w_i is the positive weight corresponding to θ_i, and λ is penalty parameter. The weights can be assigned in a data-dependent way or chosen intelligently using prior knowledge. For example, in our application, the weights $w_i,\ 1 \leq i \leq p$ are assigned to be proportional to the distance of the ocean location from the land location.

The weighted Lasso estimator is equivalent to the adaptive Lasso estimator (Zou 2006), except for the procedure used to define the weights $w_i,\ 1 \leq i \leq p$. While prior work has focused on analysis of the adaptive Lasso estimator in the asymptotic setting (Zou 2006; Huang, Ma, and Zhang 2008), we derive results for the weighted Lasso estimator in the non-asymptotic setting. The results can also be suitably extended to the adaptive Lasso estimator.

Assumptions: Consider data generated according to the linear model $y_i = \langle x_i, \theta^* \rangle + \epsilon_i,\ 1 \leq i \leq n$ and θ^* is estimated using the weighted Lasso estimator. The rows of the design matrix $X \in \mathbb{R}^{n \times p}$ are independent sub-Gaussian random vectors with sub-Gaussian norm bounded by L and covariance matrix $\Sigma = E[x_i x_i^T]$. The noise $\epsilon_i \in \mathbb{R},\ 1 \leq i \leq n$ is mean-zero i.i.d. sub-gaussian noise with sub-Gaussian norm less than 1. Assume the following,

1. The true parameter θ^* is s-sparse. Let $w^{\uparrow}$ denote the weight vector with elements in ascending order. We assume that the weights corresponding to the s non-zero elements in θ^* are among the smallest m weights $w^{\uparrow}_{1:m}$ in w. Also, let $\hat{\theta} = \theta^* + \Delta = \theta^* + \mathcal{M}(\Delta) + \mathcal{M}^{\perp}(\Delta)$, where $\Delta = \hat{\theta} - \theta^*$ is the error vector, $\mathcal{M}$ is the subspace, to which the m elements in θ^* corresponding to the weights $w^{\uparrow}_{1:m}$ belongs, and

Table 1: Description of the Earth System Models used in the experiments.

Model name	Origin	Reference
CMCC-CESM	Centro Euro-Mediterraneo per I Cambiamenti Climatici (Italy)	(Fogli et al. 2009)
INM-CM4	Institute for Numerical Mathematics (Russia)	(Volodin, Dianskii, and Gusev 2010)
MIROC5-r1i1p1	Atmosphere and Ocean Research Institute, National Institute for Environmental Studies, Japan Agency for Marine-Earth Science and Technology, University of Tokyo (Japan)	(Watanabe et al. 2010)

$\mathcal{M}^{\perp}$ is the orthogonal subspace.
2. When penalty parameter λ satisfies

$$\lambda \geq c' * \max\left\{\frac{\sqrt{m}}{\sqrt{n}\|w^{\uparrow}_{1:m}\|_2}, \frac{\sqrt{\log p}}{\sqrt{n}\tilde{w}_{\min}}\right\}, \qquad (2)$$

where $c' > 0$ is a constant,and $\tilde{w}_{\min}$ is the minimum element in $\mathcal{M}^{\perp}(w^{\uparrow})$, the error set is

$$E_r = \{\Delta \in \mathbb{R}^p | R(\mathcal{M}^{\perp}(\Delta)) \leq \beta \|w^{\uparrow}_{1:m}\|_2 \|\mathcal{M}(\Delta)\|_2\}, \qquad (3)$$

where $\beta > 1$ is a constant and $R(\theta) = \sum_{i=1}^{p} w_i|\theta_i|$. The restricted eigenvalue (RE) condition (Bickel, Ritov, and Tsybakov 2009) is assumed to be satisfied.

Theorem 1. *Under the above assumptions, the following bound holds on the error vector $\Delta = \hat{\theta} - \theta^*$ with high probability for some positive constant c,*

$$\|\Delta\|_2 \leq \frac{c}{\sqrt{n}}\left(\sqrt{m} + \frac{\|w^{\uparrow}_{1:m}\|_2\sqrt{\log p}}{\tilde{w}_{\min}}\right). \qquad (4)$$

Remark 1. *For Lasso $w_i = 1,\ 1 \leq i \leq p$. Hence in the context of the above result we recover the non-asymptotic estimation error of Lasso (Chandrasekaran et al. 2012; Negahban et al. 2012; Bickel, Ritov, and Tsybakov 2009) by substituting $m = s$, $\|w^{\uparrow}_{1:m}\|_2 = \sqrt{s}$ and $\tilde{w}_{\min} = 1$.*

Remark 2. *If the s lowest weights in $w^{\uparrow}$ correspond to the non-zero weights in θ^* then we note that $m = s$ and $\|w^{\uparrow}_{1:s}\|_2/\tilde{w}_{\min} \leq \sqrt{s}$ thus giving an improvement over the corresponding bound for Lasso.*

Remark 3. *If we end up assigning the largest weights to the non-zero elements in θ^* then $m = p$ and we recover the bound $\|\Delta\|_2 \leq \sqrt{p/n}$ which is equivalent to performing ordinary least squares on the dataset.*

The weighted Lasso problem can be numerically optimized by converting it to a Lasso problem by rescaling the data with the weights (Zou 2006).

Land Temperature Prediction

We analyze relationships between land temperature and SST in Earth system model (ESM) data. ESMs are numerical models representing physical processes in the ocean, cryosphere and land surface with data generated using simulations with different initial conditions (Taylor, Stouffer, and Meehl 2012; Pachauri et al. 2014).

We use data from the historical runs of 3 ESMs (see Table 1) included as part of the core set of experiments in CMIP5 (Taylor, Stouffer, and Meehl 2012). The historical runs of CMIP5 ESMs try to replicate observed climate conditions from 1850-2005 closely, capturing effects from changes in atmospheric CO_2 due to both anthropogenic and volcanic influences, solar forcing, land use, etc. Each monthly ESM dataset has SST data over a 2.5° × 2.5° resolution grid of earth and corresponding monthly surface temperature over land locations. In effect for each ESM we have 1872 data points with 5881 ocean locations. Brazil, Peru, and Southeast Asia are selected as the 3 land target regions to study in this paper as they are known to have diverse geological properties (Steinhaeuser, Chawla, and Ganguly 2011b).

Experiment Setting

We divide the data into 10 training sets by applying a moving window of 100 years with a stride of 5 years. The 10 years subsequent to the end of the training set are used for testing. We deseasonalize each training-test set combination separately by z-scoring each month data with the corresponding monthly mean and standard deviation. Note that both train and test sets are z-scored using monthly means and standard deviations computed from the training set. We compare the performance of weighted Lasso against the following baseline methods:

1. ℓ_1 penalized least squares (**Lasso**) (Tibshirani 1996): This is equivalent to setting all weights in weighted Lasso equal to 1.
2. Principal Component Regression (**PCR**) (Jolliffe 2011): A popular method in climate science where principal components computed from training data are considered as covariates for ordinary least square regression on response variables.
3. Gradient Boosted Trees (**GBT**) (Chen and Guestrin 2016): An ensemble method which uses decision tree as its weak learner. GBTs are implemented in Python using **xgboost** package (Chen and Guestrin 2016).
4. Deep neural networks (**Deep nets**) (LeCun, Bengio, and Hinton 2015) Multilayer perceptrons with many hidden layers and CNNs. All networks are implemented in Python using **Keras** package (Chollet 2015).

The models are evaluated quantitatively on test sets based on two metrics: (a) the root mean square error (RMSE), defined as RMSE $= \sqrt{\sum_{i=1}^{n}(\hat{y}_i - y_i)^2/n}$; (b) the coefficient of the determination (R^2), given by $R^2 = 1 - \sum_{i=1}^{n}(y_i -$

Table 2: Comparison of RMSE on test sets for land climate prediction of Brazil, Peru and South-east Asia using weighted Lasso and other baseline methods. Average RMSE ± standard error on test sets are shown. The minimum average RMSE for each target region is shown as bold. Weighted Lasso achieves overall best performance. Furthermore, linear model weighted Lasso and Lasso both outperform Deep nets and GBT.

Model	Location	Weighted Lasso	Lasso	PCR	Deep nets	GBT
CMCC -CESM	Brazil	$\mathbf{0.6580 \pm 0.0344}$	0.6681 ± 0.0317	0.8629 ± 0.0654	0.8151 ± 0.0364	0.7354 ± 0.0377
	Peru	$\mathbf{0.6901 \pm 0.0269}$	0.7120 ± 0.0214	0.8541 ± 0.0560	0.8476 ± 0.0283	0.7400 ± 0.0251
	SE Asia	$\mathbf{0.5217 \pm 0.0103}$	0.5284 ± 0.0109	0.7252 ± 0.0544	0.7424 ± 0.0153	0.5774 ± 0.0171
INM -CM4	Brazil	$\mathbf{0.7641 \pm 0.0173}$	0.7753 ± 0.0161	1.2030 ± 0.0637	0.9144 ± 0.0304	0.8707 ± 0.0193
	Peru	$\mathbf{0.7127 \pm 0.0144}$	0.7202 ± 0.0101	1.1879 ± 0.0654	0.8785 ± 0.0228	0.8164 ± 0.0184
	SE Asia	$\mathbf{0.7719 \pm 0.0171}$	0.7742 ± 0.0174	1.2751 ± 0.0645	0.9986 ± 0.0290	0.8970 ± 0.0218
MIROC5 -r1i1p1	Brazil	$\mathbf{0.5395 \pm 0.0258}$	0.5614 ± 0.0266	0.7214 ± 0.0566	0.6822 ± 0.0263	0.6005 ± 0.0279
	Peru	$\mathbf{0.5441 \pm 0.0331}$	0.5764 ± 0.0350	0.7654 ± 0.0581	0.6979 ± 0.0227	0.5953 ± 0.0262
	SE Asia	$\mathbf{0.5092 \pm 0.0154}$	0.5308 ± 0.0164	0.8139 ± 0.0712	0.7500 ± 0.0187	0.5758 ± 0.0098

Table 3: Comparison of R^2 on test sets for land climate prediction of Brazil, Peru and South-east Asia using weighted Lasso and other baseline methods. Average R^2 ± standard error on test sets is shown. The maximum average R^2 for each target region is shown as bold. Weighted Lasso achieves overall best predictive performance. Furthermore, linear model weighted Lasso and Lasso both outperform Deep nets and GBT.

Model	Location	Weighted Lasso	Lasso	PCR	Deep nets	GBT
CMCC -CESM	Brazil	$\mathbf{0.4887 \pm 0.0555}$	0.4697 ± 0.0595	0.1372 ± 0.0982	0.2292 ± 0.0633	0.3706 ± 0.0587
	Peru	$\mathbf{0.4044 \pm 0.0357}$	0.3655 ± 0.0333	0.1004 ± 0.0704	0.1018 ± 0.0476	0.3168 ± 0.0336
	SE Asia	$\mathbf{0.6963 \pm 0.0205}$	0.6901 ± 0.0188	0.4086 ± 0.0763	0.3763 ± 0.0509	0.6312 ± 0.0222
INM -CM4	Brazil	$\mathbf{0.1855 \pm 0.0342}$	0.1616 ± 0.0340	-1.098 ± 0.2387	-0.1650 ± 0.0639	-0.0629 ± 0.0550
	Peru	$\mathbf{0.3457 \pm 0.0324}$	0.3334 ± 0.0258	-0.8853 ± 0.2447	-0.0034 ± 0.0680	0.1372 ± 0.0498
	SE Asia	$\mathbf{0.3131 \pm 0.0262}$	0.3091 ± 0.0266	-0.8827 ± 0.1583	-0.1498 ± 0.0568	0.0727 ± 0.0372
MIROC5 -r1i1p1	Brazil	$\mathbf{0.7615 \pm 0.0369}$	0.7413 ± 0.0390	0.5878 ± 0.0616	0.6263 ± 0.0423	0.7146 ± 0.0330
	Peru	$\mathbf{0.7609 \pm 0.0300}$	0.7331 ± 0.0326	0.5120 ± 0.0843	0.5964 ± 0.0503	0.7186 ± 0.0256
	SE Asia	$\mathbf{0.7436 \pm 0.0298}$	0.7224 ± 0.0309	0.2949 ± 0.1448	0.4584 ± 0.0409	0.6794 ± 0.0260

$\hat{y}_i)^2/\sum_{i=1}^{n}(y_i - \bar{y})^2$, where for the i-th data point, y_i is the true normalized land temperature for a target region and $\hat{y}_i$ is the corresponding estimated value. $\bar{y}$ is the average value for all n data points. The hyperparameters for weighted Lasso (regularization parameter), Lasso (regularization parameter), PCR (number of principal components for regression) and GBT (learning rate and maximum depth of tree) are selected by validation set. Specifically, in each training set we select the first 80 years to train the model and use the next 20 years as a validation set. The hyperparameters giving best performance on the validation set are chosen. We then refit the predictive models on the full training set using the chosen hyperparameters. For GBT, we fix the number of trees to 100, and perform a grid-search to find the optimal learning rate and maximum depth of tree. For all models the optimal value of learning rate on the validation set varies between 0.05 and 0.07 and the optimal maximum tree depth is found to be 3. For Deep nets we experiment with various combinations of: (a) the number of hidden layers, (b) the number of hidden units in each layer, (c) different mini-batch size when training using the Adam optimization algorithm (Kingma and Ba 2014), and (d) ℓ_1, ℓ_2 and no regularization. Each network uses Relu (Nair and Hinton 2010) as activation function. The maximum number of epochs for training is set as 150. We also use early-stopping by examining validation set error. In almost all cases, an 8 hidden layer Deep nets with ℓ_1 regularization on the weights gave the best performance on the validation set. We report results with mini batch size set to 32. We also run experiments with transfer learning (Yosinski et al. 2014) for Convolutional Neural Networks (CNN) (Lecun et al. 1998) by training only the last two layers of the Resnet-50 (He et al. 2016) which is pre-trained on ImageNet (Russakovsky et al. 2015). Resnet-50 is found to have worse performance in comparison to Deep nets and hence, in the interest of brevity and space, we exclude it from the comparison. More details on the performance of Resnet-50 can be found in Table 6.

Experimental Results

We compare different baseline methods against weighted Lasso using average RMSE and R^2 over test sets. We also show an in-depth analysis of the performance of Deep nets for our application.

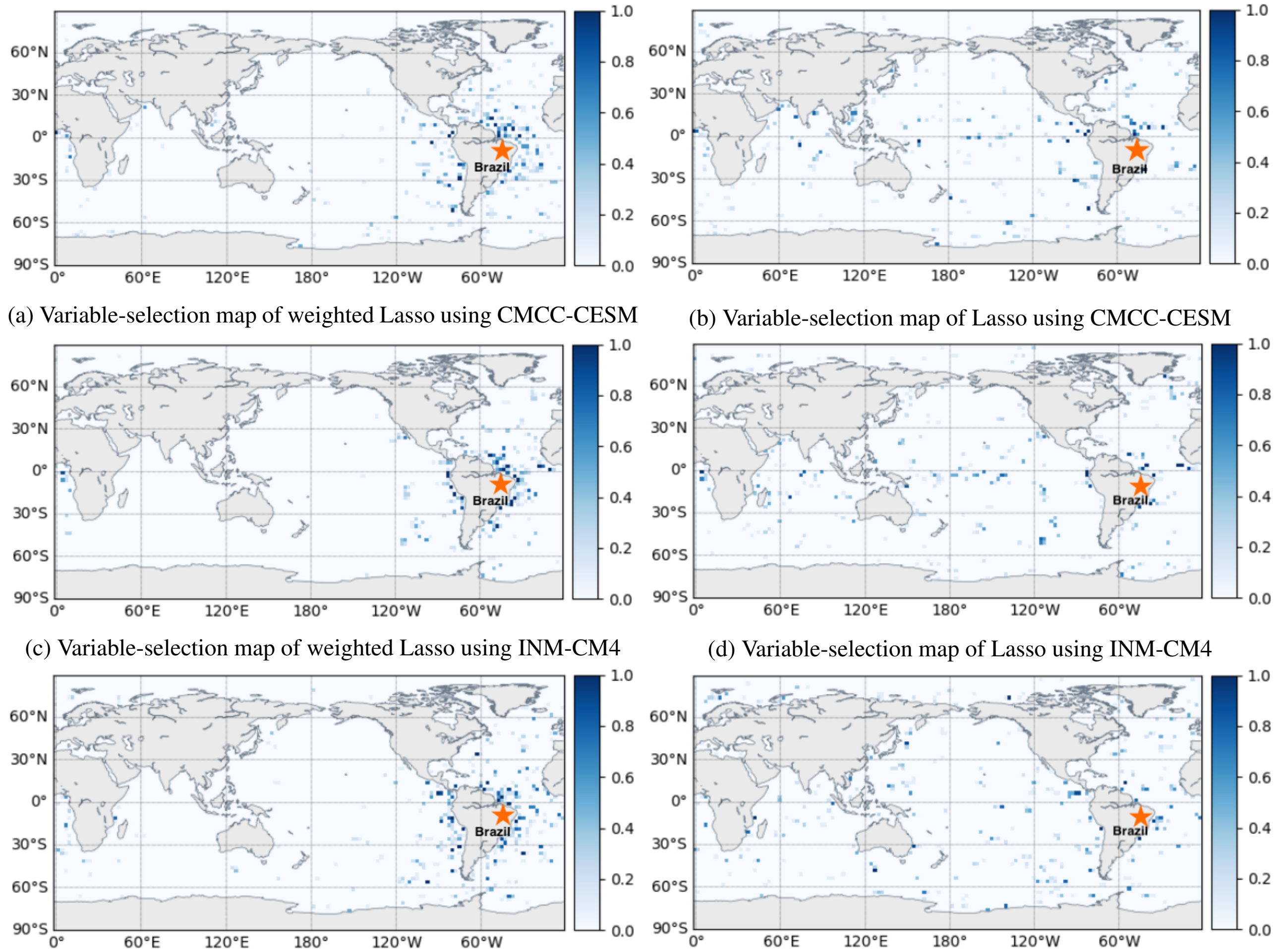

(a) Variable-selection map of weighted Lasso using CMCC-CESM

(b) Variable-selection map of Lasso using CMCC-CESM

(c) Variable-selection map of weighted Lasso using INM-CM4

(d) Variable-selection map of Lasso using INM-CM4

(e) Variable-selection map of weighted Lasso using MIROC5

(f) Variable-selection map of Lasso using MIROC5

Figure 1: Comparison of variable selection by Lasso and weighted Lasso for Brazil temperature prediction. The plot shows the probability that each ocean location is selected in the 10 runs for each ESM model. In contrast to Lasso, weighted Lasso chooses more ocean locations closer to Brazil and achieves more consistent variable selection.

Prediction Accuracy Table 2 and Table 3 report the average RMSE, R^2, and their standard errors. Weighted Lasso achieves better average predictive accuracy compared to other baseline methods across all 3 ESMs. The p-values of 2-sample K-S test (Daniel 1978) for RMSE on test sets are shown in Table 4. Weighted Lasso is significantly better than PCR, Deep nets and GBT ($p < 0.05$) in most cases (21 out of 27). While the prediction accuracy of weighted Lasso is not significantly better than Lasso, we show that weighted Lasso consistently chooses a subset of variables of which ocean locations are close to the land target region, which is more interpretable in climate science perspective.

Variable selection Weighted Lasso and Lasso introduce sparsity in variable selection. During the training phase, an ocean location is considered selected, if it has a corresponding non-zero coefficients. The behavior of weighted Lasso (and Lasso respectively) is similar for land climate prediction across 3 land target regions. We analyze the ocean locations selected by Lasso and weighted Lasso for Brazil temperature prediction for all ESM models as an example. Figure 1 plots for each ESM model the number of times each location is selected across the 10 runs. We make two observations from the plots: (a) weighted Lasso assigns non-zero weights to ocean location close to Brazil consistent with domain knowledge, and (b) variable selection in weighted Lasso is more stable compared to Lasso in the sense that the same locations are picked in all 10 datasets. However, Lasso has few variables which are consistently chosen in all predictive models for the same land target region. Also, the frequently selected variables using Lasso are distributed at arbitrary locations, which is not interpretable in climate science perspective. We also compare the weights from a unit from the first layer in Deep nets in Figure 2. Deep nets assign non-zero weights for all ocean locations even with ℓ_1 regularization.

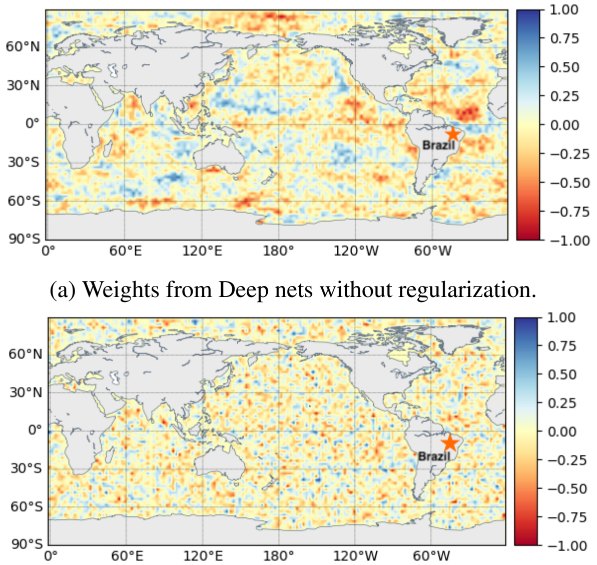

(a) Weights from Deep nets without regularization.

(b) Weights from Deep nets with ℓ_1 regularization.

Figure 2: Comparison of regression coefficients of a unit from Deep nets with and without ℓ_1 regularization for Brazil. All weights are normalized to $[-1, 1]$ by dividing the largest value among absolute weights.

Deep nets: What happened?

In this section, we analyze various facets of the performance of Deep nets. The performance of Deep nets is influenced by the number of hidden layers, number of hidden units, mini-batch size, regularization etc. We analyze the impact of each of these on the performance of Deep nets by varying one of the parameters while keeping the others fixed. We also demonstrate that Deep nets overfit the training data and hence do not generalize well on the test set.

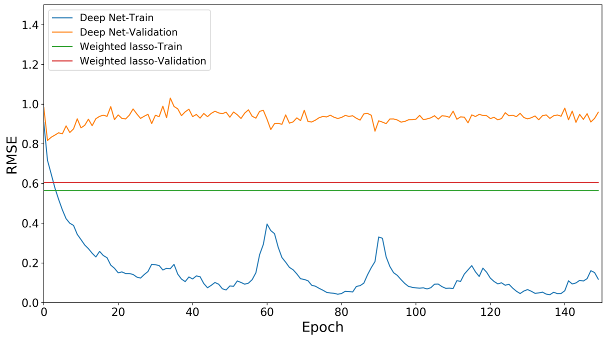

Figure 3: An example of model overfitting during the training phase for Deep nets. Deep nets are trained for 150 epochs. The blue curve and orange curve indicate the RMSE of the training and validation set for Deep nets. There is a clear gap between the training and validation RMSE. The RMSE of weighted Lasso on both training (green line) and validation (red line) sets are also shown for comparison.

Overfitting Figure 3 shows the training and validation set RMSE after each epoch for a 8 layer Deep nets with 32 hidden units trained for temperature prediction over Brazil. The Deep nets training error stabilizes after about 20 epochs and is lower than the RMSE of linear models. In contrast the validation set error of the Deep nets is much higher which indicates that Deep nets overfit the noise in the training set and hence can not generalize well over the unseen test set.

Effect of number of hidden units Figure 4 plots the test RMSEs for temperature prediction over Brazil as we alter the number of hidden units in each layer. The RMSE slightly decreases as the number of hidden units increases from 1 to 64 for both shallow networks with 1 hidden layer, and Deep nets with 8 hidden layers.

Table 4: The p-values from 2-sample KS-test on RMSE of test sets of weighted Lasso against other baseline methods are shown. The p-values less than 0.05 are shown in bold. The performance of weighted Lasso is significantly better than non-linear baseline methods for most of target regions.

Model	Location	Lasso	PCR	Deep nets	GBT
CMCC -CESM	Brazil	0.9747	0.1108	**0.0310**	0.1108
	Peru	0.6750	0.3128	**0.0068**	0.3128
	SE Asia	0.6750	**0.0001**	**0.0000**	**0.0068**
INM -CM4	Brazil	0.6750	**0.0001**	**0.0012**	**0.0012**
	Peru	0.9747	**0.0000**	**0.0000**	**0.0068**
	SE Asia	0.9747	**0.0000**	**0.0001**	**0.0068**
MIROC5 -r1i1p1	Brazil	0.9747	**0.0339**	**0.0120**	0.1473
	Peru	0.6750	0.1108	**0.0120**	0.3743
	SE Asia	0.6750	**0.0000**	**0.0000**	**0.0120**

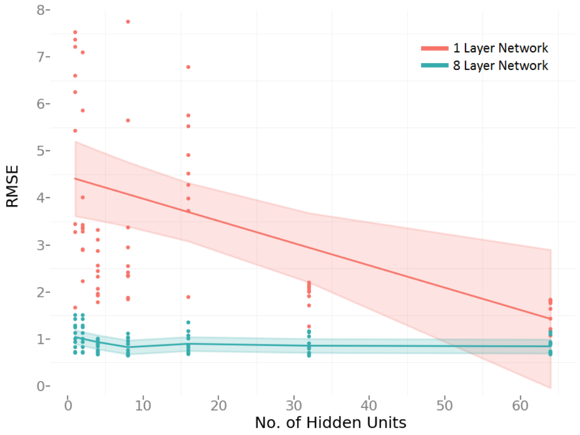

Figure 4: Average RMSE on test sets vs number of hidden units for Brazil temperature prediction with CMCC-CESM. The shaded zone indicates the lower and upper confidence intervals (95%) around the predicted mean. For both 1-Layer and 8-Layer network configuration, the RMSE tends to slightly decrease with increasing number of hidden units.

Shallow vs Deep Structure Figure 5 compares Deep nets with 1 hidden layer against Deep nets with 8 hidden layers on test set prediction over Brazil. Having more layers gives better test set RMSE.

Table 5: Comparison of RMSE on test sets of regularized Deep nets and weighted Lasso. Average test RMSE ± standard error are shown. Deep nets with ℓ_1 regularization has smaller test set RMSE than ℓ_2 and $\ell_1 + \ell_2$ regularization.

Model	Location	Weighted Lasso	Deep nets	Deep nets with ℓ_1	Deep nets with ℓ_2	Deep nets with $\ell_1 + \ell_2$
CMCC-CESM	Brazil	$\mathbf{0.6580 \pm 0.0344}$	0.8151 ± 0.0364	0.6931 ± 0.0260	0.8458 ± 0.0744	1.0635 ± 0.1308
	Peru	$\mathbf{0.6901 \pm 0.0269}$	0.8476 ± 0.0283	0.7499 ± 0.0210	0.9099 ± 0.0374	1.2099 ± 0.0453
	SE Asia	$\mathbf{0.5217 \pm 0.0103}$	0.7424 ± 0.0153	0.5656 ± 0.0063	0.6869 ± 0.0215	0.8992 ± 0.0324
INM-CM4	Brazil	$\mathbf{0.7641 \pm 0.0173}$	0.9144 ± 0.0304	0.8453 ± 0.0185	0.7334 ± 0.0403	1.0992 ± 0.1232
	Peru	$\mathbf{0.7127 \pm 0.0144}$	0.8785 ± 0.0228	0.7815 ± 0.0119	0.7193 ± 0.0390	1.1686 ± 0.0964
	SE Asia	$\mathbf{0.7719 \pm 0.0171}$	0.9986 ± 0.0290	0.8585 ± 0.0204	0.7891 ± 0.0600	1.2414 ± 0.1042
MIROC5-r1i1p1	Brazil	$\mathbf{0.5395 \pm 0.0258}$	0.6822 ± 0.0263	0.5919 ± 0.0160	0.9884 ± 0.0278	1.2544 ± 0.0477
	Peru	$\mathbf{0.5441 \pm 0.0331}$	0.6979 ± 0.0227	0.5848 ± 0.0358	0.8781 ± 0.0177	1.5395 ± 0.1526
	SE Asia	$\mathbf{0.5092 \pm 0.0154}$	0.7500 ± 0.0187	0.5616 ± 0.0194	0.9887 ± 0.0458	1.3306 ± 0.0949

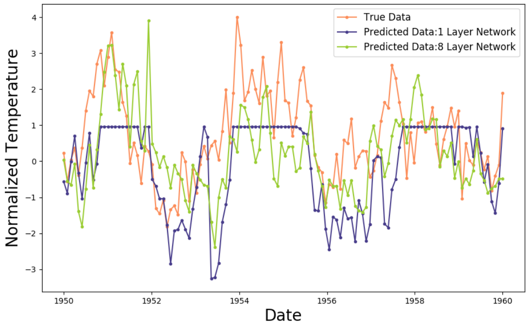

Figure 5: The comparison of predicted land temperatures in Brazil with CMCC-CESM over a 10 year period (1950-1960) between a shallow and a deep network structure. The deep structure predictions are better than a shallow network.

Table 6: Comparison of the best RMSEs among weighted Lasso, Deep nets, and Resnet-50 using data from CMCC-CESM. Resnet-50 shows worse predictive accuracy compared to other methods.

Location	Weighted Lasso	Deep nets	Resnet-50
Brazil	$\mathbf{0.6513 \pm 0.0635}$	0.8151 ± 0.0364	1.2972 ± 0.4109
Peru	$\mathbf{0.6944 \pm 0.0444}$	0.8476 ± 0.0283	1.3739 ± 0.3211
SE Asia	$\mathbf{0.5162 \pm 0.0213}$	0.7424 ± 0.0153	1.4760 ± 0.4227

Effect of mini-batch size Mini-batch size while training is believed to have a strong impact on Deep nets performance (Bengio 2012; Masters and Luschi 2018). We analyze the effect on average test RMSE of mini-batch size for temperature prediction over all three land locations (Figure 6). The RMSE are highest with small batch sizes, steadily decreasing with increasing batch size.

Effect of Regularization We explore 3 regularization schemes, ℓ_1, ℓ_2 and $\ell_1 + \ell_2$. Table 5 shows the comparison on the test RMSE values of weighted Lasso and Deep nets before and after applying ℓ_1, and ℓ_2 regularization. ℓ_1 regularization seems to give better performance over other regularization schemes including no regularization.

Conclusions

In this paper, we propose a weighted Lasso scheme for prediction on spatial climate data in order to encode the inherent spatial information in such datasets. Also, the non-asymptotic estimation error bound for weighted Lasso is given. The proposed method is evaluated on a task to predict temperature for 3 distinct land target regions using SST from the historical runs of 3 ESMs. The weights are set to be proportional to the geographical distance between the ocean location of each predictor and the target land region, constraining the estimator to pick spatially nearby ocean locations. Weighted Lasso not only achieves better prediction accuracy compared to other linear and non-linear models, including PCR, GBT and Deep nets across all ESMs, but also selects stable predictors consistent with domain knowledge.

We also conduct a comprehensive analysis of Deep nets on high-dimensional climate datasets with small sample size. Empirical results show that linear models outperform the non-linear models and thus are more suitable for climate problems where the number of samples is limited.

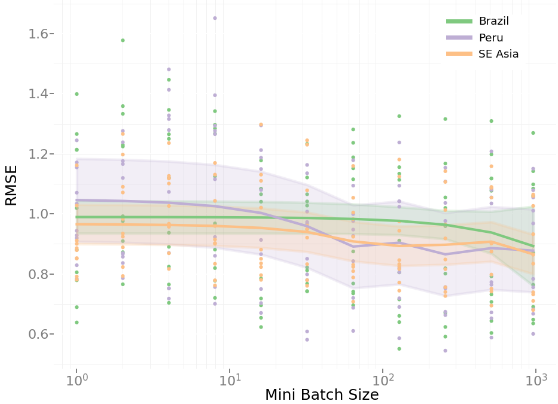

Figure 6: Average test RMSE vs mini batch size over Brazil, Peru, and SE Asia for ESM model CMCC. Mini batch size of 1, 2, 4, 8, 16, 32, 64, 128, 256, 512 as well as full batch size are used on a 8 hidden layer network. The average RMSE on test sets decreases as batch size increases.

Acknowledgments

The research was supported by NSF grants IIS-1563950, IIS-1447566, IIS-1447574, IIS-1422557, CCF-1451986, IIS-1029711.

References

Aalto, J.; Pirinen, P.; Heikkinen, J.; and Venäläinen, A. 2013. Spatial interpolation of monthly climate data for finland: comparing the performance of kriging and generalized additive models. *Theoretical and Applied Climatology* 112(1-2):99–111.

Bengio, Y. 2012. *Practical Recommendations for Gradient-Based Training of Deep Architectures*. Berlin, Heidelberg: Springer Berlin Heidelberg. 437–478.

Bickel, P. J.; Ritov, Y.; and Tsybakov, A. B. 2009. Simultaneous analysis of lasso and dantzig selector. *The Annals of Statistics,* 1705–1732.

Chandrasekaran, V.; Recht, B.; Parrilo, P. A.; and Willsky, A. S. 2012. The convex geometry of linear inverse problems. *Foundations of Computational mathematics,* 12(6):805–849.

Chatterjee, S.; Steinhaeuser, K.; Banerjee, A.; Chatterjee, S.; and Ganguly, A. 2012. Sparse group lasso: Consistency and climate applications. In *Proceedings of the 2012 SIAM International Conference on Data Mining (SDM)*, 47–58.

Chen, T., and Guestrin, C. 2016. Xgboost: A scalable tree boosting system. In *Proceedings of the 22nd ACM SIGKDD International Conference on Knowledge Discovery and Data Mining (SIGKDD)*, 785–794.

Chollet, F. 2015. Keras. https://github.com/fchollet/keras.

Daniel, W. W. 1978. *Applied nonparametric statistics*. Houghton Mifflin.

DelSole, T., and Banerjee, A. 2017. Statistical seasonal prediction based on regularized regression. *Journal of Climate,* 30(4):1345–1361.

Fogli, P. G.; Manzini, E.; Vichi, M.; Alessandri, A.; Patara, L.; Gualdi, S.; Scoccimarro, E.; Masina, S.; and Navarra, A. 2009. Ingv-cmcc carbon (icc): A carbon cycle earth system model. *CMCC Research Paper,* 61:31.

Francis, R., and Renwick, J. 1998. A regression-based assessment of the predictability of new zealand climate anomalies. *Theoretical and Applied Climatology,* 60(1):21–36.

Goovaerts, P. 1999. Geostatistics in soil science: state-of-the-art and perspectives. *Geoderma* 89(1-2):1–45.

He, K.; Zhang, X.; Ren, S.; and Sun, J. 2016. Deep residual learning for image recognition. In *Proceedings of the IEEE conference on computer vision and pattern recognition (CVPR)*, 770–778.

Hsieh, W. W., and Tang, B. 1998. Applying neural network models to prediction and data analysis in meteorology and oceanography. *Bulletin of the American Meteorological Society,* 79(9):1855–1870.

Huang, J.; Ma, S.; and Zhang, C.-H. 2008. Adaptive lasso for sparse high-dimensional regression models. *Statistica Sinica,* 1603–1618.

Jolliffe, I. 2011. Principal component analysis. In *International encyclopedia of statistical science*. Springer. 1094–1096.

Kingma, D. P., and Ba, J. 2014. Adam: A method for stochastic optimization. *arXiv preprint arXiv:1412.6980*.

Krizhevsky, A.; Sutskever, I.; and Hinton, G. E. 2012. Imagenet classification with deep convolutional neural networks. In *Advances in neural information processing systems (NIPS)*, 1097–1105.

LeCun, Y.; Bengio, Y.; and Hinton, G. 2015. Deep learning. *Nature,* 521(7553):436.

Lecun, Y.; Bottou, L.; Bengio, Y.; and Haffner, P. 1998. Gradient-based learning applied to document recognition. *Proceedings of the IEEE,* 86(11):2278–2324.

Masters, D., and Luschi, C. 2018. Revisiting small batch training for deep neural networks. *arXiv preprint arXiv:1804.07612*.

McDermott, P. L., and Wikle, C. K. 2017. Bayesian recurrent neural network models for forecasting and quantifying uncertainty in spatial-temporal data. *arXiv preprint arXiv:1711.00636*.

Nair, V., and Hinton, G. E. 2010. Rectified linear units improve restricted boltzmann machines. In *Proceedings of the 27th international conference on machine learning (ICML)*, 807–814.

Negahban, S. N.; Ravikumar, P.; Wainwright, M. J.; and Yu, B. 2012. A unified framework for high-dimensional analysis of m-estimators with decomposable regularizers. *Statistical Science* 27(4):538–557.

O'Brien, G.; O'Keefe, P.; Rose, J.; and Wisner, B. 2006. Climate change and disaster management. *Disasters* 30(1):64–80.

Olivieri, A. C. 2018. *Introduction to Multivariate Calibration: A Practical Approach*. Springer.

Pachauri, R. K.; Allen, M. R.; Barros, V. R.; Broome, J.; Cramer, W.; Christ, R.; Church, J. A.; Clarke, L.; Dahe, Q.; Dasgupta, P.; et al. 2014. *Climate change 2014: synthesis report. Contribution of Working Groups I, II and III to the fifth assessment report of the Intergovernmental Panel on Climate Change*. IPCC.

Russakovsky, O.; Deng, J.; Su, H.; Krause, J.; Satheesh, S.; Ma, S.; Huang, Z.; Karpathy, A.; Khosla, A.; Bernstein, M.; Berg, A. C.; and Fei-Fei, L. 2015. Imagenet large scale visual recognition challenge. *International Journal of Computer Vision,* 115(3):211–252.

Steinhaeuser, K.; Chawla, N.; and Ganguly, A. 2011a. Comparing predictive power in climate data: Clustering matters. *Advances in Spatial and Temporal Databases,* 39–55.

Steinhaeuser, K.; Chawla, N. V.; and Ganguly, A. R. 2011b. Complex networks as a unified framework for descriptive analysis and predictive modeling in climate science. *Statistical Analysis and Data Mining,* 4(5):497–511.

Taylor, K. E.; Stouffer, R. J.; and Meehl, G. A. 2012. An overview of cmip5 and the experiment design. *Bulletin of the American Meteorological Society,* 93(4):485–498.

Tibshirani, R. 1996. Regression shrinkage and selection via the lasso. *Journal of the Royal Statistical Society,* 267–288.

Vandal, T.; Kodra, E.; Ganguly, S.; Michaelis, A.; Nemani, R.; and Ganguly, A. R. 2017. Deepsd: Generating high resolution climate change projections through single image super-resolution. In *Proceedings of the 23rd ACM SIGKDD International Conference on Knowledge Discovery and Data Mining (SIGKDD)*, 1663–1672.

Volodin, E.; Dianskii, N.; and Gusev, A. 2010. Simulating present-day climate with the inmcm4.0 coupled model of the atmospheric and oceanic general circulations. *Atmospheric and Oceanic Physics,* 46(4):414–431.

Walter, C.; McBratney, A. B.; Douaoui, A.; and Minasny, B. 2001. Spatial prediction of topsoil salinity in the chelif valley, algeria, using local ordinary kriging with local variograms versus whole-area variogram. *Soil Research* 39(2):259–272.

Watanabe, M.; Suzuki, T.; Oishi, R.; Komuro, Y.; Watanabe, S.; Emori, S.; Takemura, T.; Chikira, M.; Ogura, T.; Sekiguchi, M.; et al. 2010. Improved climate simulation by miroc5: mean states, variability, and climate sensitivity. *Journal of Climate,* 23(23):6312–6335.

Yosinski, J.; Clune, J.; Bengio, Y.; and Lipson, H. 2014. How transferable are features in deep neural networks? In *Advances in neural information processing systems (NIPS)*, 3320–3328.

Zou, H. 2006. The adaptive lasso and its oracle properties. *Journal of the American statistical association,* 101(476):1418–1429.